

## Electronic Supporting Information

### Functionalization of polyacrylamide with MoS<sub>2</sub> nanoflakes for use in transient photodetector

Arpit Verma, Priyanka Chaudhary, Ravi Kant Tripathi, B.C.Yadav\*

Nanomaterials and Sensors Research Laboratory, Department of Physics,  
Babasaheb Bhimrao Ambedkar University, Lucknow-226025, U.P., India

\*Email: [balchandra\\_yadav@rediffmail.com](mailto:balchandra_yadav@rediffmail.com)

#### 1. Characterization techniques:

The JEOL, JSEM- 6490 LV system of Oxford Instruments was used for the SEM analysis. X-ray analysis was done by using X-ray diffractometer (X'Pert Pro PANalytical, Netherland) by CuK<sub>α</sub> radiation ( $\lambda=1.54 \text{ \AA}$ ). Nanoflakes of MoS<sub>2</sub> are analyzed by the High Resolution Transmission Electron Microscope (TEM) Model: FP 5022/22-Tecnai G2 20 S-TWIN. FTIR spectra were recorded by the Thermo-Scientific (Nicole 6700) between the ranges of 400-4000 cm<sup>-1</sup>. The Raman analysis was done by Renishaw using 514.5 nm Ar<sup>+</sup> with power 15 mW. PL was carried out by Horiba Fluorolog FL3-11. The thermo-gravimetric (TG) and differential thermal (DT) analysis were carried out by the (PERKINELMER STA 6000). UV-Visible spectra are analyzed by the Thermo-Scientific (Evolution 201) spectrophotometer in the range of 190-1100 nm. The Keithley source meter (6517 B) was used for the analysis of the photodetector device.

#### 2. Fabrication of the photodetector device:

For this purpose, the ITO substrate was cleaned by some chemical reagents such as DI water, isopropyl alcohol and acetone. The ultrasonication was used for sonicating the ITO substrate for 20 min with each reagent and the cleaned ITO was dried in a programmable oven for 30 min at 60°C. The homogeneous aqueous solution of MoS<sub>2</sub> and MoS<sub>2</sub>-Polyacrylamide metallopolymer were used for the fabrication of the device to the application of photodetector. The solution was

deposited on the ITO substrate by spin coating method at 1000 rpm for 60s. The fabricated device was dried at the hot plate for 30 min at 50°C. Silver contacts were painted by masking technique with the channel width 2 mm and 4 mm height followed by drying at 50°C for 1 hour in the oven.

### 3. XRD Analysis:

From the XRD analysis it can be concluded that nanoflakes are well dispersed in the polymer matrix. Bragg's law (relation S1) is used for calculating for the inter-planar spacing (d) of the prepared sample.

$$2d\sin\theta_{hkl} = n\lambda, \text{ where } n = 1 \quad \text{S(1)}$$

Induced stress and strain<sup>1</sup> of the prepared materials were calculated by the following relations S(2) and S(3). The length of the dislocation line per unit volume is termed as the dislocation density ( $\delta$ )<sup>2</sup>, which has been estimated by the relation S(4). All the XRD parameters are given in table S1

$$\text{Stress } (S) = \frac{\lambda}{L\sin\theta_{hkl}} - \frac{\beta}{\tan\theta_{hkl}} \quad \text{S(2)}$$

$$\text{Strain } (\varepsilon) = \frac{\beta\cos\theta_{hkl}}{4} \quad \text{S(3)}$$

$$\text{Dislocation density } (\delta) = \frac{1}{L^2} \quad \text{S(4)}$$

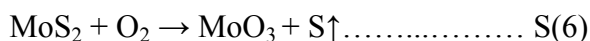
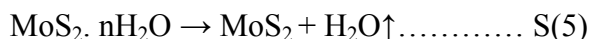
**Table S1. XRD analysis data for MoS<sub>2</sub> and MoS<sub>2</sub>-Polyacrylamide metallopolymer**

Material	2θ (Deg)	The crystallite size (nm)	FWHM (degree)	Inter- planar spacing d (Å)	Stress (S)	Strain (ε) ×10 <sup>-3</sup>	Dislocation density (line/m <sup>3</sup> ) ×10 <sup>15</sup>
MoS <sub>2</sub>	14.08	18.99	0.43	6.31	0.0064	7.36	2.77
MoS <sub>2</sub> -Poly-	14.76	10.84	0.74	6.02	0.0112	3.21	8.51

acrylamide							
------------	--	--	--	--	--	--	--

#### 4. Thermo-gravimetric Analysis of MoS<sub>2</sub>:

The TG graph of the MoS<sub>2</sub> shows a weight loss in the range of 32 to 100<sup>o</sup>C attributes to the loss the adsorbed humidity on the sample. The weight became stable until temperature was 350<sup>o</sup>C after this a quick weight loss found between 350-500<sup>o</sup>C, which mainly attributes to the conversion of MoS<sub>2</sub> to MoO<sub>3</sub> exhibits an endothermic peak in the differential thermal signals. No significant weight loss found in the range of 500 to 530<sup>o</sup>C but after this a sharp weight loss peak is found which attributes to the melting of oxidized MoO<sub>3</sub><sup>3-5</sup>.



#### 5. Optical characterization:

UV-Visible spectra of the MoS<sub>2</sub> nanoflakes show four characteristic peaks A, B, C and D at the 653, 591, 435 and 396nm respectively. A direct transition peak at the K point observed at the 700nm<sup>6</sup>. The high absorption at the A and B peaks supports the association of these peaks with direct transitions<sup>7</sup>. C and D peaks around 500nm represent transition from the deep of the valence band, which is previously reported by Mishra et al.<sup>6</sup>. Photoluminescence spectra exhibited the excitation peak of the MoS<sub>2</sub> nanoflakes at the 360nm and the emission peak is 647nm which shows the energy gap 1.91eV. In the FTIR spectra of the MoS<sub>2</sub> nanoflakes, the characteristic peak of the Mo-S vibration is found around 608.5 cm<sup>-1</sup>. The other peaks at the 1637 and 3444cm<sup>-1</sup> corresponds to the bending and stretching vibration of the hydroxyl group. A small Raman shifting is observed from MoS<sub>2</sub> nanoflakes to MoS<sub>2</sub>-Polyacrylamide.

#### 6. Photodetection mechanism:

The photoresponse (%) can be expressed by the relation S(7) with the help of photocurrent (I<sub>p</sub>) and dark current (I<sub>d</sub>)<sup>2</sup>.

$$\text{Photoresponse (\%)} = \frac{I_p - I_d}{I_d} \times 100 \% \quad \text{S(7)}$$

The transient photoresponse of the material is governed by the trap depth energy and the recombination centers present in the mid gap states of the material as well as desorption of the O<sub>2</sub> molecule under the illumination. Thus, this can be suggested that a poor response of the photodetector can be accredited as the more defected states, recombination centers as well as trap levels.

Adsorption and desorption of the oxygen molecules on the surface as well as on grain boundaries of the prepared sample is the cause of the photodetection. Under the ambient atmospheric conditions the oxygen molecules present in the environment adsorbed on the sample and grain boundaries. These oxygen molecules take out the conduction band electrons and convert them into the oxygen ions<sup>8</sup>, as shown in the chemical reactions S(8) (a and b).



When the conduction band electron goes to the valence band a depletion region of the lower conductivity is created, which results in the increased potential barrier height ( $\phi = eV_s$ ) due to upward bending of the conduction and valence band edges. By the relation S(9) it is clear that depletion region will cause the lower carrier concentration.<sup>9</sup>

$$W_D = \sqrt{\frac{2 \epsilon \phi_B}{N_d e^2}} \quad \text{S(9)}$$

where  $N_d$  and  $\epsilon$  is the donor density and the permittivity of the prepared metallopolymeric nanomaterial. The current flowing in this condition is the dark current and this is controlled by the

barrier potential ( $V_s$ ) created by the adsorption of the oxygen molecules on the grain boundaries of the material. This current is expressed by the relation S(10).

$$I = I_0 \exp\left(-\frac{eV_s}{kT}\right) = I_0 \exp\left(-\frac{\Phi_B}{kT}\right) \quad \text{S(10)}$$

When the illumination is switched ON with the energy of higher than bandgap energy of the material, the charge carriers are ejected from the grain boundaries and also from the surface of the sample. These opposite charge photogenerated ions neutralized the oxygen ions, which finally get liberated as the oxygen molecules. In this process the electrons from the valence band excited and moves towards the conduction band whereas depletion layer also decreases which causes high rate of current flow. This high conductivity path provides a pathway for the higher photoresponse<sup>10</sup> which can be expressed as relation S(11).

$$\text{Photoresponse} = \exp\left(\frac{-\Delta\Phi_B}{kT}\right) = \exp\left(\frac{-e\Delta V_s}{kT}\right) \quad \text{S(11)}$$

where,  $\Delta V_s$  and  $\Delta\Phi_B$  are the change in surface potential on exposure of light and potential barrier height.

The trap states and recombination centers present in the band gap region is responsible for the rise and fall of the photoresponse under applied illumination<sup>11</sup>. In the illumination, the electrons which are liberated from the valence band trapped in the recombination centers present in the band states and on further illumination these recombined electrons also ejected from the trap states at the lower energy than the band gap of the material. Thus, high level of the trap states and defects present on the surface of the sample results poor photoresponse.

As it is seen from the current-voltage (I-V) characteristics that current in the pure MoS<sub>2</sub> nanoflakes is of 10<sup>-10</sup> Ampere order. Responsivity and detectivity of the MoS<sub>2</sub> nanoflakes based photodetector are found to 0.1773 mA/W and 5.2503×10<sup>10</sup> Jones. Other parameters of photodetector are given in table S(2) and S(3).

**Table S2. Photodetector parameter of MoS<sub>2</sub> nanoflakes:**

Power	I <sub>p</sub> (A)	I <sub>d</sub> (A)	Area (mm <sup>2</sup> )	λ (nm)	on off ratio (I <sub>p</sub> /I <sub>d</sub> )	Responsivity (mA/W)	LDR (dB)	%EQE at 365 nm	Detectivity (Jones)	NEP (W)
40 μW/cm <sup>2</sup>	4.2774×10 <sup>-10</sup>	2.1390×10 <sup>-12</sup>	3×2	365	199.971	0.1773	46.0194	0.0601	5.2503×10 <sup>10</sup>	1.2062×10 <sup>-8</sup>

**Table S3. Photodetector parameter of polyacrylamide:**

Power	I <sub>p</sub> (A)	I <sub>d</sub> (A)	Area (mm <sup>2</sup> )	λ (nm)	on off ratio (I <sub>p</sub> /I <sub>d</sub> )	Responsivity (mA/W)	LDR (dB)	%EQE at 365 nm	Detectivity (Jones)	NEP (W)	No. of peak
40 μW/cm <sup>2</sup>	6.2783×10 <sup>-9</sup>	8.0584×10 <sup>-10</sup>	3×2	365	7.79099	2.2802	17.831	0.7731	3.4781×10 <sup>10</sup>	3.5341×10 <sup>-7</sup>	1 st peak
40 μW/cm <sup>2</sup>	3.6183×10 <sup>-9</sup>	8.0584×10 <sup>-10</sup>	3×2	365	4.49005	1.1718	13.045	0.3973	1.7885×10 <sup>10</sup>	6.8767×10 <sup>-7</sup>	2 nd peak
40 μW/cm <sup>2</sup>	2.2371×10 <sup>-9</sup>	8.0584×10 <sup>-10</sup>	3×2	365	2.77612	0.5964	8.8688	0.2022	9.0978×10 <sup>10</sup>	1.3513×10 <sup>-6</sup>	3 rd peak

**Table S4. Photodetector parameter of MoS<sub>2</sub>-Polyacrylamide:**

Power	I <sub>p</sub> (A)	I <sub>d</sub> (A)	Area (mm <sup>2</sup> )	λ (nm)	on off ratio (I <sub>p</sub> /I <sub>d</sub> )	Responsivity (mA/W)	LDR (dB)	%EQE at 365 nm	Detectivity (Jones)	NEP (W)
2.3 mW/cm <sup>2</sup>	4.4331×10 <sup>-7</sup>	2.7480×10 <sup>-9</sup>	3×2	365	161.3210	3.1924	44.1538	1.0824	2.6371×10 <sup>10</sup>	8.6077×10 <sup>-7</sup>
375 μW/cm <sup>2</sup>	2.5279×10 <sup>-7</sup>	2.7480×10 <sup>-9</sup>	3×2	365	91.9905	11.1129	39.2749	3.7677	9.1796×10 <sup>10</sup>	2.4728×10 <sup>-7</sup>
40 μW/cm <sup>2</sup>	1.4697×10 <sup>-7</sup>	2.7480×10 <sup>-9</sup>	3×2	365	53.4825	60.0925	34.5642	20.3738	4.9638×10 <sup>11</sup>	4.5730×10 <sup>-8</sup>

**References:**

- 1 B. D. Cullity, *Elements of X-ray Diffraction*, Addison-Wesley Publishing, 1956.
- 2 V. Kumar, I. Rawal, V. Kumar and P. K. Goyal, *Phys. B Phys. Condens. Matter*, 2019, **575**, 411690.
- 3 L. Chang, H. Yang, J. Li, W. Fu, Y. Du, K. Du, Q. Yu, J. Xu and M. Li, *Nanotechnology*, 2006, **17**, 3827.
- 4 X. Feng, X. Wang, W. Xing, K. Zhou, L. Song and Y. Hu, *Compos. Sci. Technol.*, 2014, **93**, 76–82.
- 5 R. Wei, H. Yang, K. Du, W. Fu, Y. Tian, Q. Yu, S. Liu, M. Li and G. Zou, *Mater. Chem. Phys.*, 2008, **108**, 188–191.
- 6 A. K. Mishra, K. V Lakshmi and L. Huang, *Sci. Rep.*, , DOI:10.1038/srep15718.
- 7 J. P. Wilcoxon, P. P. Newcomer and G. A. Samara, *J. Appl. Phys.*, 1997, **81**, 7934–7944.

- 8 S. Singh, A. Bhaduri, R. K. Tripathi, K. B. Thapa, R. Kumar and B. C. Yadav, *Sol. Energy*, 2019, **188**, 278–290.
- 9 D. A. Neamen, *Semiconductor physics and devices : basic principles*, New York, NY: McGraw-Hill, 2012.
- 10 S. Jeon, I. Song, S. Lee, B. Ryu, S. Ahn, E. Lee, Y. Kim, A. Nathan, J. Robertson and U. Chung, *Adv. Mater.*, 2014, **26**, 7102–7109.
- 11 M. Rani and S. K. Tripathi, *Renew. Sustain. Energy Rev.*, 2016, **61**, 97–107.